Loss of CO_2-induced Distensibility in Cerebral Arteries with Chronic Hypertension or Vasospasm after Subarachnoid Hemorrhage

SEIJI NAKAJIMA[1], TAKESHI KONDOH[1], AKITSUGU MORISHITA[1], HARUO YAMASHITA[1], EIJI KOHMURA[1], TAKASHI SAKURAI[2], KOICHI YOKONO[2], and KEIJI UMETANI[3]

Department of [1]Neurosurgery and [2]Internal and Geriatric Medicine, Graduate School of Medicine, Kobe University, Kobe, Japan
[3]Japan Synchrotron Radiation Research Institute, SPring-8, Sayo-gun, Hyogo, Japan

Abbreviations: ICA, internal carotid artery; MCA, middle cerebral artery; ACA, anterior cerebral artery; ECA, external carotid artery; CCA, common carotid artery; MAP, mean arterial pressure; PCA, posterior cerebral artery; BA, basilar artery

    We developed a rat cerebral angiography system using monochromatic synchrotron radiation X-rays at SPring-8, a third generation synchrotron radiation facility. Using new technique, we assessed the distensibility of major trunk arteries after subarachnoid hemorrhage (SAH) in normotensive and hypertensive rats. Twenty-five adult Wistar Kyoto rats (WKY) and fourteen stroke-prone spontaneously hypertensive rats (SHR) were prepared SAH by double hemorrhage injection method into cisterna magna. Angiography was performed on day 7 and was repeated three times in each rat before and after loading of hypercapnia at 100-120 mmHg of $PaCO_2$. The diameters of major trunk vessels were assessed. Light microscopic observation of artery lumen and wall were also performed. Angiographical vasospasm was demonstrated in basilar artery in WKY with 66 % reduction in diameter of control. In ICA and other major trunk in WKY and all the arteries in SHR did not demonstrate vasospasm. SHA resulted in loss of hypercapnia-induced distention in BA of WKY. In SHR, the distensibility was impaired regardless of hemorrhage. Histological study demonstrated basilar artery in WKY thickened at 184 % after SAH and became similar to non-hemorrhagic SHR. ICA in WKY and both BA and ICA in SHR were unchanged in wall thickness before and after SAH. High quality angiography demonstrated deteriorated distensibility in chronic hypertension or SAH-induced spastic vessels.

    Subarachnoid hemorrhage (SAH) is often associated with a delayed vasospasm that is a major course of disability in patients after cerebral aneurysm rupture. Many researchers have used rodents to study the pathogenesis of cerebral vasospasm after SAH because small animals are less expensive and easy to handle. Rat models were developed in which blood was injected directly into the cisterna magna (3, 24). The degree of vasospasm is determined by measurement of the vessel diameters and direct observation through cranial

bone window was used initially (2). Subsequently, angiography has been reported in rat SAH model, however, it is very difficult because of the small size of the animal. Furthermore, physiological change cannot be characterized as it has in models using other larger species.

Recently, we have developed a microangiography system using monochromatic synchrotron radiation X-rays at SPring-8, a third generation synchrotron radiation facility. With this system at SPring-8, high spatial resolution of 8 µm has been achieved using phantoms. We have firstly applied this system for cerebral microangiography in rats and mice (9, 13, 16, 25). In the present study, we have focused on in vivo assessment of spastic rat cerebral arteries after SAH. Impaired autoregulation of the cerebral blood flow has been known in rat SAH model between 2 and 5 days after SAH (20). This study was done with133-Xenon injection into carotid artery and reflected pathogenesis of small arteriole in the cortex. The major artery trunks, that are targets of interventional approach in patients, were not shown yet in previous studies. Using microangiography technique, we studied the change of distensibility of those major artery trunks by loading systemic hypercapnia.

Secondly, we studied the effects of chronic hypertension on vasospasm using spontaneously hypertensive rats (SHR). Chronic hypertension in SHR induces thick media in cerebral arteries in comparison with normotensive rats (15) and may affect the spastic change as well as distensibility in systemic hypercapnia. Although aging is known to increase the degree of vasospasm after SAH in rabbits, studies with chronic hypertension has not been done yet.

MATERIALS AND METHODS

Imaging System and Animal Preparation

All experimental procedures followed the guidelines for animal experimentations at Kobe University Graduate School of Medicine. The imaging was performed at the 2nd optical hatch of BL28B2 beamline at SPring-8 (Japan Synchrotron Radiation Research Institute) in Hyogo, Japan. Details of the imaging system used in the present study were, in part, previously described (13, 16).

Adult Wistar Kyoto rat (WKY, n=25) and adult SHR (n=14), weighting between 450 and 600g, aged 6 months, were used. The method to produce SAH is based on a double hemorrhage injection method. On day 0, rats were anesthetized with pentobarbital sodium (50 mg/kg, i.p.) and allowed to breath spontaneously. Under sterile condition, rats were held in a 20° head down in a stereotaxic frame and the atlano-occipital membrane was exposed. A 27-gauge needle bent at the tip for a length of 2 mm was carefully inserted into the cisterna magna. On day 2, rats were anesthetized again and a second SAH was induced as described above. On day 7, imaging study was performed under pentobarbital sodium (50 mg/kg, i.p.) anesthesia, which has been reported in our previous reports (13, 16).

Experimental Protocol

After the animal preparation was completed, the PE-50 tube inserted into the ECA was connected to an automated injector (Nihon Koden, Japan) that was programmed to reproducibly deliver nonionic contrast media (Iomeprol) at 0.2 ml / 0.4 sec for ICA imaging and 0.5 ml / 1.0 sec for BA. This injection volume and speed were determined based on our pilot study, in which different volumes of the contrast media were injected at different injection rates to obtain the most acceptable and physiological images. Arterial blood gases were checked before the first imaging. The first angiogram was performed to estimate the basal tone of the vessels. We allowed at least 3-min intervals between angiograms to reestablish physiological blood flow before each angiographic study.

The inhalation of CO_2 at 12-15 % mixed in air was performed for 6 minutes. An angiogram, at the end of inhalation, was then performed. The arterial blood gases were analyzed and the inhalation was returned to normal air. An additional angiogram was performed at 10 min under normocapnia, and the arterial blood gases were analyzed. Rats were divided into four subgroups; a) WKY with SAH (n=17), b) WKY without SAH (n=5), c) SHR with SAH (n=9), d) SHR without SAH (n=8). Rats in group b) and d) were as control in which saline was injected into cisterna magnum instead of autologous blood.

Image Analysis

The images were stored digitally. The initial acquisition time for an image was 30 images per second. To make the subtraction images, ten original images were added and subtracted by the pre-infusion image. The vessel diameter was measured semiautomatically on the digital image with readymade software (Image ProPlus, U.S.A.) combined with a program developed for this study. A short temporary axis was delineated by hand at the vessels specified for measurement. The axis was delineated within 0.5 mm after branching for PCA, MCA and ACA. For ICA, the axis was in the middle of the segment between PCA and MCA. BA was measured at two points of one third proximal and one third distal. The density profile perpendicular to the temporary axis was calculated and distance between these two peaks of phase refractions of X-ray on the border of vessel wall was measured as a diameter of the vessel.
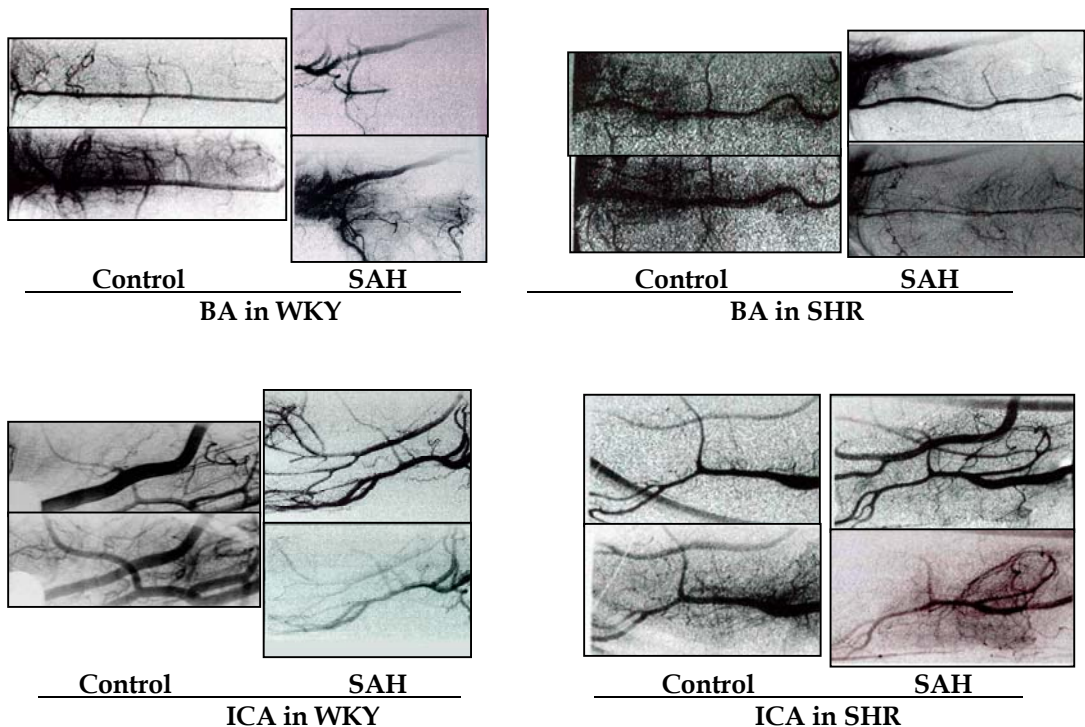

Figure 1: Representative images of rat cerebral vessels taken by SPring-8 and micorangiography technique. Uppper: normocapnia, lower: hypercapnia.   BA: basilar artery, ICA: internal carotid artery, SHR: spontaneously hypertensive rat, WKY: Wistar Kyoto rat, SAH: subarachnoid hemorrhage.

Morphometric study

After angiography, rats were killed by overdose anesthesia and decapitated. Rats were perfused transcardially by 4% parahormaldehyde in phosphate buffer for 30 minutes. Brain were removed and soaked in 10 % parahormaldehyde for 7days. After paraffin embedding, slices containing basilar artery and internal carotid artery was made at the thickness of 10 μm and stained with hematoxylin and eosin.   The internal diameter and wall thickness of the arteries were measured using a digitized image analysis system. The thickness was defined as the distance from the luminal surface to the outer border of the media at four different points.

Statistics

Data are presented as means +/- S.E.. An unpaired Student *t* test was used to detect significant differences when two groups were compared. Statistical differences among group means were determined by one-way ANOVA with repeated measures, followed by a post hoc comparison. A value of *P*< 0.05 was considered to be statistically significant.

| **Control** | **SAH** | **Control** | **SAH** |
| **BA in WKY** | | **BA in SHR** | |

| **Control** | **SAH** | **Control** | **SAH** |
| **ICA in WKY** | | **ICAin SHR** | |
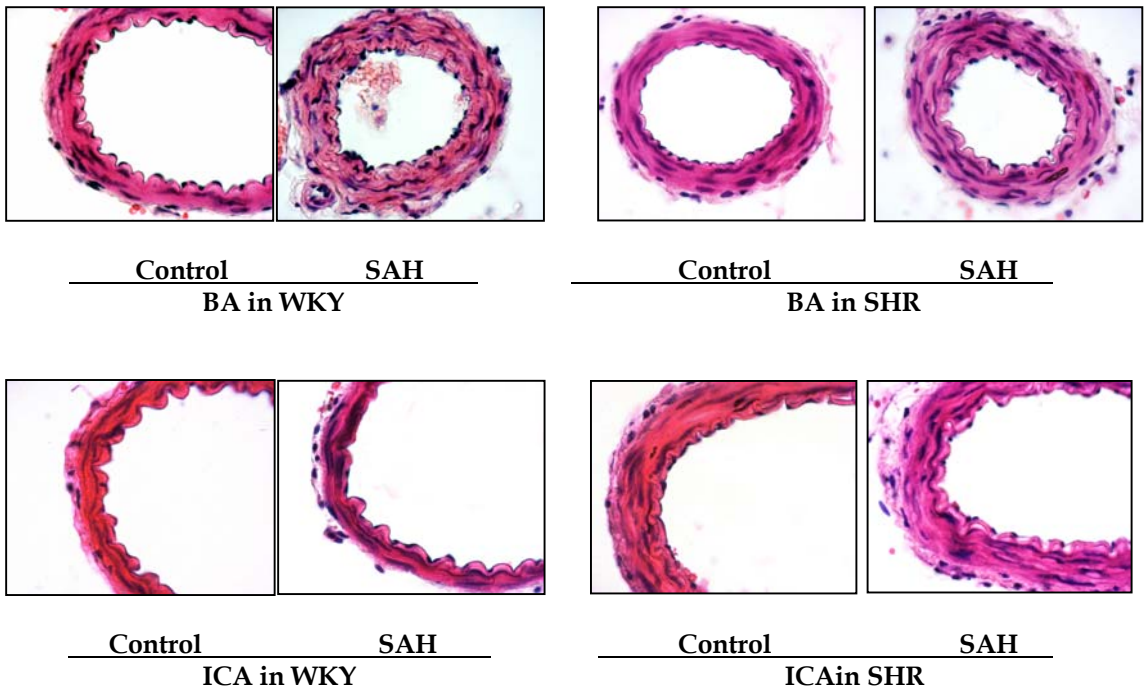
Figure 2: Histological demonstration of cross section in basilar arteries and internal carotid arteries.

RESULTS

With our experimental setting of 0.2 ml injection, the posterior fossa was not filled by the contrast media indicating selective ICA angiography was performed. Within the radiation field of 3 x 7.3 mm, the images of major trunk vessels of ICA from the entry point to intracranial space, PCA, MCA and ACA were consistently obtained. The posterior choroidal artery, the large branch of PCA was also within the field but it was always associated with overlapping images of thalamic branches in the axial view and this made analysis impossible. The image of posterior communication artery arising from the PCA was occasionally obtained by selective ICA angiography but mostly faint.

The vessel diameters of rats without SAH (SAH(-)) and rats with SAH(SAH(+)) measured by angiography were summarized in Table 1. In SAH(-) rats, the diameters of BA were significantly narrower in SHR than in WKY (132 μm vs.248 μm at proximal and 102 μm vs. 274 μm at distal; $p < 0.05$) and other major trunk vessels did not significantly differ between WKY and SHR. In SAH(+) rats, significant vasospasm was observed in BA of WKY (64-66 % of SAH(-)). Other major trunk vessels in SAH(+) WKY and all of the major trunk vessels in SAH(+) SHR-SP had no spastic changes (81-139 % of SAH(-)).

By loading CO_2, all of the trunk vessels in SAH(-) WKY demonstrated significant dilatation (125 –169 % of pre-CO_2 values for each) (Table 2). This dilatation ability was lost after SAH except PCA. In SHR, both SAH(-) and SAH(+) did not demonstrated vasodilatation by CO_2 loading at all.

The histological measurement of ICA and BA before SAH demonstrated significant narrower diameter in SHR compared with WKY (110 μm vs. 153 μm in BA and 218 μm vs. 297 μm in ICA) as shown in Table 3. SAH-induced narrowing of the vessels was not observed histologically in all. The measurement of arterial wall thickness demonstrated that in SAH(-) rats, both BA and ICA had significantly thicker wall in SHR compared with WKY (29.6 μm vs. 19.2 μm in BA and 33.3 μm vs. 29.2 μm in ICA). SAH-induced-pathological change was observed only in BA of WKY, in which arterial wall significantly thickened by SAH (181 % of SAH(-)). This thickened value of the diameter in BA of WKY was comparable to BA of SHR.

Table 1. Comparative measurments in WKY and SHR with subarachnoid hemorrhage

	vessel diameter (μm)		Spasm (%)	p Value
	SAH(-)	SAH(+)		
Basilar A.(proximal)				
WKY	248±21.3	164±34.7	66	0.02
SHR	132±33.1	149±32.3	112	NS
Basilar A.(distal)				
WKY	274±26.7	176±36.1	64	0.02
SHR	102±41.8	124±36.1	121	NS
ICA				
WKY	319±28.1	360±39.2	113	NS
SHR	340±27.7	306±37.5	99	NS
MCA				
WKY	214±30.3	235±21.5	109	NS
SHR	218±15.9	217±14.7	99	NS
ACA				
WKY	255±20.3	208±27.1	81	NS
SHR	226±18.6	226±21.2	100	NS
PCA				
WKY	180±28.5	251±15.0	139	NS
SHR	220±46.6	212±26.7	97	NS

Table 2. CO2 induced distention of trunk vessels in the chronic vasospasm

	WKY				SHR			
	SAH(-)		SAH (+)		SAH(-)		SAH (+)	
	mean±SE (%)	p value	mean±SE (%)	p value	mean±SE (%)	p value	mean±SE (%)	p value
Basilar A.(proximal)								
pre	238±21.3 (100)	P=0.04	164±34.7 (100)	NS	132±33.1 (100)	NS	148±32.3 (100)	NS
post	294±27.9 (125)		151±35.1 (99.7)		172±46.3 (130)		165±37.5 (11.5)	
rec/10min	236±37.7 (99.1)		145±51.6 (88.7)		155±48.2 (117)		152±46.6 (102)	
Basilar A.(distal)								
pre	268±26.7 (100)	P=0.03	176±36.1 (100)	NS	102±41.8 (100)	NS	124±36.1 (100)	NS
post	368±43.2 (137)		161±42.5 (91.1)		128±56.5 (133)		141±54.8 (114)	
rec/10min	294±51.4 (108)		140±49.1 (79.2)		170±49.5 (133)		114±69.8 (91.7)	
ICA								
pre	319±28.1 (100)	P=0.0001	390±27.4 (100)	NS	340±27.8 (100)	NS	306±37.5 (100)	NS
post	385±23.4 (121)		455±34.7 (117)		353±29.6 (104)		382±48.8 (125)	
rec/10min	338±37.5 (106)		375±26.2 (96.1)		317±43.3 (93.1)		234±9.3 (76.4)	
MCA								
pre	214±22.4 (100)	P=0.01	235±21.5 (100)	NS	218±15.9 (100)	NS	216±14.7 (100)	NS
post	298±19.5 (139)		229±40.3 (97.4)		250±26.5 (115)		245±13.4 (113)	
rec/10min	201±26.1 (93.9)		223±40.8 (94.9)		210±15.3 (96.3)		158±5.8 (72.8)	
ACA								
pre	255±20.3 (100)	P=0.04	226±22.7 (100)	NS	226±18.6 (100)	NS	226±21.2 (100)	NS
post	282±32.4 (110)		265±24.2 (117)		230±20.8 (102)		274±19.4 (121)	
rec/10min	260±23.1 (102)		205±22.3 (87.2)		200±15.3 (88.5)		182±24.8 (80.5)	
PCA								
pre	180±28.5 (100)	P=0.01	251±15.0 (100)	p=0.007	220±46.6 (100)	NS	212±26.7 (100)	NS
post	226±19.7 (126)	P=0.007	313±18.4 (125)		207±41.0 (93.9)		258±18.8 (122)	
rec/10min	226±8.4 (145)		257±24.3 (102)		160±30.6 (72.7)		166±28.9 (78.1)	

Table 3. Comparative measurments in normal rats and SHR with subarachnoid hemorrhage

	WKY			SHR		
	SAH(-)	SAH(+)	p Value	SAH(-)	SAH(+)	p Value
Basilar A						
vessel wall(μm)	19.16±0.17	34.82±1.28	p=0.002	29.58±0.67	31.25±0.98	NS
vessel lumen(μm)	153.33±6.89	151.79±9.57	NS	110±7.29	83.33±5.00	NS
ICA						
vessel wall(μm)	29.16±0.83	29.29±1.08	NS	33.33±0.33	35.25±0.56	NS
vessel lumen(μm)	296.67±32.0	272.5±13.08	NS	217.5±10.79	197±14.26	NS

DISCUSSION

Angiographical Assessment of Vasospasm in Rodents

Measurements of rat cerebral arteries after subarachnoid hemorrhage have been reported using angiography (3, 8, 11, 17, 27), and observation with a cranial window (18, 22, 23). By mammographic equipment or selective biplane digital subtraction angiography systems, recent studies using rodents showed availability of measuring the vessel diameters with or without spasms (11, 26).

Magnification of the vessels using a mammography suggests the possibility of visualizing the small cerebral vessels (11, 12, 17). The small focus technique provides high geometric magnification with longer film - focus distance. This technique is especially useful in combination with digital subtraction techniques. They demonstrated the ability to view rat cerebral trunk arteries and some extracranial arteries including superior and inferior ophthalmic arteries, although the vessel diameters were not measured. The theoretical magnification of the mammography was suggested to be x 250 in the literature, however, one

concern with magnification increases, is radiation scattering which makes the margins of vessel image blurry.

Regarding the time resolution for rat cerebral angiography, some studies used anterograde injection of the contrast media by placing the cannula in CCA or ICA, thus the ipsilateral blood flow in ICA was disrupted (11, 12). With this preparation, the volumes of injected contrast media were between 0.2 to 0.3 ml. The obtained images showed cross filling of the contrast media to the whole contralateral hemisphere as well as the posterior fossa, suggesting that normal intracranial blood flow was absolutely changed at the time of imaging. Others used retrograde injection via the ECA to the CCA (17). An external carotid perfusion loop allows for the introduction of the contrast medium without changing perfusion pressure or flow in the cerebral hemisphere. However, the injection volume of the contrast media was as high as 0.5 ml and only a single angiography was performed in one experimental setting.

In the present study, we demonstrated the ability to obtain rat cerebral microangiograms using synchrotron radiation. Selective microangiography of hemispheric brain clearly showed not only the images of major trunk vessels but also of vessels less than 100 μm in diameter. The subtraction images were obtained every 0.33 sec and microangiography repeated up to five times in each rat, which is in contrast with previous studies where only two imagings could be done. This high quality of microangiography has not been reported by current conventional method of imaging. We believe that this can be obtained only by the combination of highly monochromatized SR and a new X-ray SATICON camera.

We found that the absolute value of vessel diameter in our studies was smaller than previous studies in the rat brain, in which angiography using mammography measured the diameter of the MCA in rat at 305-350 μm (11, 17). The diameter of the MCA in our study was at 201 +/- 20 μm in WKY. This diameter is close to that found in a histological study (15, 20) and we think, therefore, that our study is likely more accurate. Magnified images in mammography may have scattering radiation around the contrast media resulting in obscure margins and inaccurately larger diameter of the vessels. A large injection volume of the contrast media or proximal blocking of the ICA due to the catheter placement might cause the enlargement of the vessels that can not be detected by conventional methods used in previous studies.

Chronic Hypertension and Distensibility of Cerebral Arteries

In WKY, we observed vasospasm in basilar artery after SAH at 66% of pre-SAH diameter. The vasospasm was not observed in ICA, MCA, ACA and PCA. Actually, ICA and PCA showed a tendency of enlargement of the vessels after SAH, although which was not statistically significant (ICA: from 319 μm to 360 μm, PCA: from 180 μm to 251 μm). Interestingly, similar pattern of enlargement in ICA and PCA were observed in comparison between normotensive WKY and hypertensive SHR (ICA: 319 μm to 340 μm, PCA: 180 μm to 220 μm). We speculate that after SAH in WKY, ICA and PCA might be enlarged due to compensatory dilatation for severely affected spastic basilar artery that was mostly affected by SAH by blood injection into posterior cranial fossa. Similarly, in SHR, the basilar artery might be mostly affected because other major vessels have a collateral blood flow via the external carotid arteries.

We have demonstrated that the vasospasm was absent in basilar artery of the SHR. We suspect that the reason for absence of vasospasm was, at least in part, due to morphological change of vessel wall. In comparison of the thickness of basilar artery wall between WKY and SHR, SHR was significantly thicker than WKY (30 μm in SHR vs. 19 μm in WKY). Not only simply thick wall but also morphological changes of medial smooth muscle cells

and blood brain barrier have been reported in SHR (1, 15). Taken together, pre-existing affected distensibility in SHR might result in lack of spastic change after SAH. This may be also responsible for our observation of lack of distention by hypercapnia in SHR. The distensibility of affected vessels can be quantified only by high-resolution imaging. Regarding the impact of chronic hypertension on the distensibility of cerebral vessels, previous study using SHR and laser Doppler measurement of cerebral blood flow has been reported that pressure-dependent constriction of cerebral vessels was attenuated and lost after stroke (21). By hypercapnia, cerebral blood flow measurement by hydrogen clearance method resulted in no significant difference of the vasodilation between normotensive rats and hypertensive rats (6). Those previous studies were based on relative blood flow changes and direct measurement of the vessel diameter has never been performed. With large experimental animals, various studies have been reported but those were all non-pathological condition and no study could be done with chronic hypertension (4, 5, 7). Our study showed that major trunk vessels in SHR were less affected by SAH than in WKY, indicating that the degree of vessel damage is already maximized in SHR, leading high vulnerability. Similar result was obtained using young and aged rabbit with SAH (14).

Clinical implication of the present data

Our results in this study were mimicking of clinical observation in several points (10). Firstly, location of SAH clot is a key of induction of vasospasm, which is commonly observed in SAH patients and we found similar localized vasospasm in rodent. Secondly, the mortality of SHR after SAH was recognized high as two out of nine rats whereas zero in WKY. Pre-existing deteriorated autoregulation of the cerebral blood flow in SHR probably lead low blood perfusion in brain stem, resulting fetal ischemia under circumstances of high intracranial pressure with SAH.   Thirdly, autoregulation of cerebral blood flow is affected even in normotensive WKY, indicating maintaining of systemic blood pressure is essential to prevent delayed ischemic damage after SAH. Impaired endothelium-dependent relaxation has been discussed recently as a main reason of such pathogenesis of distensibility (26). To evaluate such a mechanisms, not only a simple measurement of vessel diameters but also imaging studies like microangiography using vasodilator is useful.

REFERENCES

1. **Amenta F., Ferrante F., Sabbatini M., and Ricci A.** 1994. Quantitative image analysis study of the cerebral vasodilatory activity of nicardipine in spontaneously hypertensive rats. Clin Exp Hypertens. **16**: 359-371.
2. **Barry K.J., Gogjian M.A., and Stein B.M.** 1979. Small animal model for investigation of subarachnoid hemorrhage and cerebral vasospasm. Stroke. **10**: 538-541.
3. **Delgado T.J., Brismar J., and Svendgaard N.A.** 1985. Subarachnoid haemorrhage in the rat: angiography and fluorescence microscopy of the major cerebral arteries. Stroke **16**: 595-602.
4. **Diringer M.N., Heffez D.S., Monsein L., Kirsch J.R., Hanley D.F., and Traystman R.J.** 1991. Cerebrovascular CO2 reactivity during delayed vasospasm in a canine model of subarachnoid hemorrhage. Stroke **22**: 367-372.

5. **Diringer M.N., Kirsch J.R., and Traystman R.J.** 1994. Reduced cerebral blood flow but intact reactivity to hypercarbia and hypoxia following subarachnoid hemorrhage in rabbits. J Cereb Blood Flow Metab **14**: 59-63.

6. **Heinert G., Casadei B., and Paterson D.J.** 1998. Hypercapnic cerebral blood flow in spontaneously hypertensive rats. J Hypertens. **16**: 1491-1498.

7. **Ishiguro M., Puryear C.B., Bisson E., Saundry C.M., Nathan D.J., Russell S.R., Tranmer B.I., and Wellman G.C.** 2002. Enhanced myogenic tone in cerebral arteries from a rabbit model of subarachnoid hemorrhage. Am J Physiol Heart Circ Physiol **283**: H2217-2225.

8. **Kader A., Krauss W.E., Onesti S.T., Elliott J.P., and Solomon R.A.** 1990. Chronic cerebral blood flow changes following experimental subarachnoid hemorrhage in rats. Stroke. **21**: 577-581.

9. **Kidoguchi K., Tamaki M., Mizobe T., Koyama J., Kondoh T., Kohmura E., Sakurai T., Yokono K., and Umetani K.** 2006. In vivo X-ray angiography in the mouse brain using synchrotron radiation. Stroke.**37**: 1856-1861.

10. **Lanzino G., Kassell N.F., Germanson T.P., Kongable G.L., Truskowski L.L., Torner J.C., and Jane J.A.** 1996. Age and outcome after aneurysmal subarachnoid hemorrhage: why do older patients fare worse? J Neurosurg **85**: 410-418.

11. **Longo M., Blandino A., Ascenti G., Ricciardi G.K., Granata F., and Vinci S.** 2002. Cerebral angiography in the rat with mammographic equipment: a simple, cost-effective method for assessing vasospasm in experimental subarachnoid haemorrhage. Neuroradiology **44**: 689-694.

12. **Luedemann W., Brinker T., Schuhmann M.U., von Brenndorf A.I., and Samii M.** 1998. Direct magnification technique for cerebral angiography in the rat. Invest. Radiol. **33**: 421-424.

13. **Morishita A., Kondoh T., Sakurai T., Ikeda M., Bhattacharjee A.K., Nakajima S., Kohmura E., Yokono K., and Umetani K.** 2006. Quantification of distension in rat cerebral perforating arteries. Neuroreport. **17**: 1549-1553.

14. **Nakajima M., Date I., Takahashi K., Ninomiya Y., Asari S., and Ohmoto T.** 2001. Effects of aging on cerebral vasospasm after subarachnoid hemorrhage in rabbits. Stroke **32**: 620-628.

15. **Nordborg C., Fredriksson K., and Johansson BB.** 1985.The morphometry of consecutive segments in cerebral arteries of normotensive and spontaneously hypertensive rats. Stroke. **16**: 313-320.

16. **Oizumi X.S., Akisaki T., Kouta Y., Song X.Z., Takata T., Kondoh T., Umetani K., Hirano M., Yamasaki K., Kohmura E., Yokono K., and Sakurai T.** 2006. Impaired response of perforating arteries to hypercapnia in chronic hyperglycemia. Kobe J Med Sci. **52**: 27-35.

17. **Piepgras A., Thome C., and Schmiedek P.** 1995. Characterization of an anterior circulation rat subarachnoid hemorrhage model. Stroke **26**: 2347-2352.

18. **Quan L., and Sobey C.G.** 2000. Selective effects of subarachnoid hemorrhage on cerebral vascular responses to 4-aminopyridine in rats. Stroke **31**: 2460-2465.

19. **Rasmussen G., Hauerberg J., Waldemar G., Gjerris F., and Juhler M.** 1992. Cerebral blood flow autoregulation in experimental subarachnoid haemorrhage in rat. Acta Neurochir (Wien). **119**: 128-133.

20. **Rieke G.K.** 1987. Thalamic arterial pattern: an endocast and scanning electron microscopic study in normotensive male rats. Am. J. Anat. **178**: 45-54.

21. **Smeda J.S., VanVliet B.N., and King S.R.** 1999.Stroke-prone spontaneously

hypertensive rats lose their ability to auto-regulate cerebral blood flow prior to stroke. J Hypertens. **17**: 1697-1705.

22. **Sobey C.G., Heistad D.D., and Faraci F.M.** 1996. Effect of subarachnoid hemorrhage on dilatation of rat basilar artery in vivo. Am J Physiol **271**: H126-132.

23. **Sobey C.G., Heistad D.D., and Faraci F.M.** 1997. Effect of subarachnoid hemorrhage on cerebral vasodilatation in response to activation of ATP-sensitive K+ channels in chronically hypertensive rats. Stroke **28**: 392-396.

24. **Solomon R.A., Antunes J.L., Chen R.Y., Bland L., and Chien S.** 1985. Decrease in cerebral blood flow in rats after experimental subarachnoid hemorrhage: a new animal model. Stroke. **16**: 58-64.

25. **Tamaki M., Kidoguchi K., Mizobe T., Koyama J., Kondoh T., Sakurai T., Kohmura E., Yokono K., and Umetani K.** 2006. Carotid artery occlusion and collateral circulation in C57Black/6J mice detected by synchrotron radiation microangiography. Kobe J Med Sci. **52**: 111-118.

26. **Weidauer S., Vatter H., Dettmann E., Seifert V., and Zanella F.E.** 2006. Assessment of vasospasm in experimental subarachnoid hemorrhage in rats by selective biplane digital subtraction angiography. Neuroradiology **48**: 176-181.

27. **Yamamoto S., Nishizawa S., Tsukada H., Kakiuchi T., Yokoyama T., Ryu H., and Uemura K.** 1998. Cerebral blood flow autoregulation following subarachnoid hemorrhage in rats: chronic vasospasm shifts the upper and lower limits of the autoregulatory range toward higher blood pressures. Brain Res **782**: 194-201.